

Modelling Keypoint Ambiguity in Domain Adaptive Animal Pose Estimation with Scaled Variation

Chang Liu

Department of System Design Engineering, University of Waterloo

chang.liu@uwaterloo.ca

1 ABSTRACT

Pose estimation suffers from inherent noisy ambiguities such as joint occlusion and inaccurate labelling. In supervised pose estimation, regression-based methods are remarkably successful in mitigating ambiguity by modelling the keypoint output as a distribution. Unsupervised domain adaptive pose estimation suffers more ambiguity and performance degradation compared to their supervised counterparts due to the compounding effects of noisy ambiguities under distributional shifts. Yet methods modelling keypoint ambiguity for unsupervised domain adaptation remain unexplored. In light of this, we propose a simple yet effective module for **Modelling keypoint Ambiguity with scaled Variation (MAV)** to capture this noise and mitigate ambiguities in keypoint predictions. Our method achieves **76.2% PCK@0.05** for the horse class in the standard animal benchmark and outperforms the state-of-the-art by **+0.7%** with few parameter overheads.

2 INTRODUCTION AND PROBLEM DEFINITION

2D pose estimation is a task estimating all 2D key points of a human, animal or object from an image. Thanks to advancements in computer vision, supervised 2D pose estimation has made significant progress in recent years and is incredibly successful in resolving ambiguities in challenging cases such as occlusions, motion blur and truncations [3].

Recently, domain adaptive pose estimation became a vital research direction [13] because manual annotation is expensive and labour-intensive [13]. Domain adaptive pose estimation focuses on

adapting knowledge from a source domain with labelled data (often synthetic) to an unlabeled target domain. However, unsupervised domain adaptive (UDA) pose estimation suffers performance degradation compared to their supervised counterparts due to data distribution shifts. Moreover, this performance degradation is further exacerbated by noisy ambiguities like motion blurs, inaccurate labelling and occlusions in both the source domain and target domain. This ambiguity is especially prominent in animal pose estimation due to the irregular and unpredictable nature of animal movements and poses.

In this work, we mitigate the noisy ambiguities in unsupervised domain adaptive animal pose estimation by adding variations to the feature representations in the decoder before the deconvolution layers. To ensure consistent noise mitigation in the target domain, 1) the latent feature vectors of the source to target images are adaptively updated with the mean and variance of the target image in

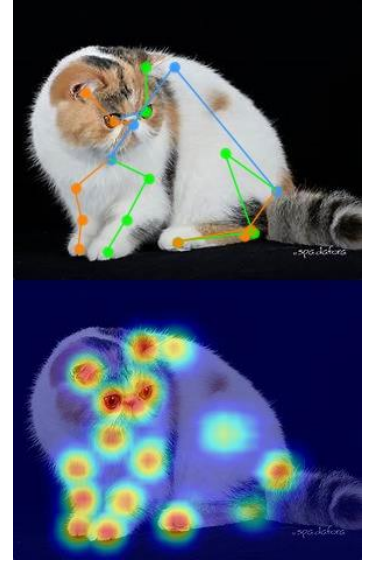


Figure 1: Unpredictable Animal Pose [2]

adaptive instance norm after the encoder, and 2) model weights are updated between the student and the teacher model by exponential moving averaging. We also experimented with adding scaled variation directly to both the soft keypoint predictions and hard keypoint predictions in the student and teacher models to accentuate the keypoint predictions.

Although specifically designed for unsupervised pose estimation, our proposed framework is general and can be adapted to both supervised and unsupervised pose estimation. We benchmarked the proposed method on the Synthetic Animal \rightarrow TigDog dataset, specifically for horses and tigers. With a simple yet effective architecture, our method achieves **76.2 Percentage of Correct Keypoints** at 5% of image resolution for horses, 0.7% higher than the previous state-of-the-art method.

Our contributions can be summarized as follows:

- We proposed a novel module for modelling keypoint ambiguity with scaled variation to capture noise and mitigate ambiguities in keypoint predictions for domain adaptive pose estimation.
- We investigated the efficacy of existing supervised noise-capturing approaches in the unsupervised problem setting and found them to be ineffective. Our proposed method mitigates this inefficacy.
- Our method is the first approach for capturing noise in unsupervised pose estimation. We show the potential of mitigating ambiguities in the unsupervised domain adaptive scenario.

3 RELATED WORK

3.1 POSE ESTIMATION

Existing pose estimation methods can be divided into two main categories, heatmap-based methods and regression-based methods. Heatmap-based methods are dominant in the field of human pose estimation. Such methods generate a likelihood heatmap for each joint and locate the joint as the point with either argmax [1, 3, 4] or soft-argmax. Regression-based methods directly map the input vector to the output joint coordinates [5]. These methods suffer from inferior performance but are fast even on edge devices. Current regression methods are vulnerable to noisy labels, occlusions, motion blur, and truncations. Hence, existing methods attempt to model the noise keypoint predictions with maximum likelihood estimates for regression-based methods [3]. Although not as severe, heatmap-based methods still suffer from the same issue. Furthermore, existing methods are all applied to supervised problems [1, 3, 4, 5] and may interfere with the soft keypoint prediction updates in unsupervised pose estimation. Our method bridges this gap by proposing a noise estimation module heatmap-based approach for unsupervised pose estimation.

3.2 NOISE-BASED APPROACH FOR DOMAIN ADAPTATION

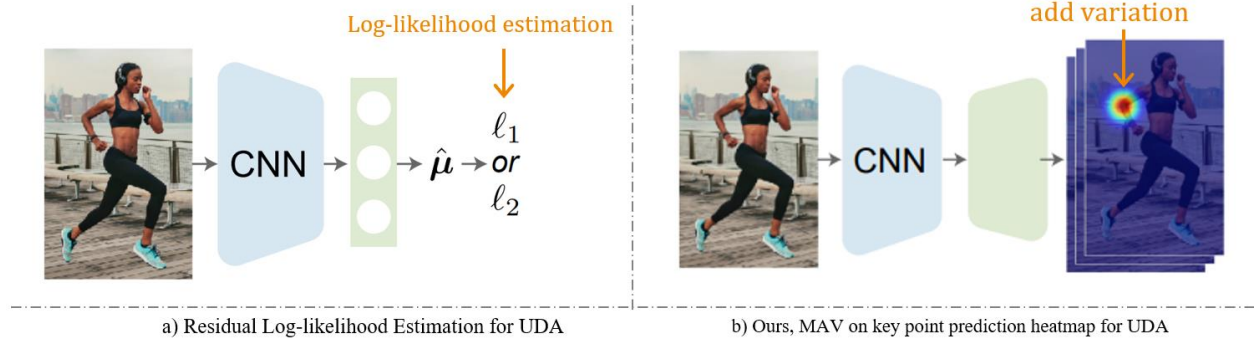
Adding noise to data during model training is a common technique that can be applied at the image or feature level. Popular methods include dropout [8], colour jittering [7], and adding Gaussian noise. Some researchers have also explored optimizing the noise added to extracted features to create adversarial examples that fool the model. Techniques such as M2m [10] and AdvProp [11] have successfully used adversarial examples to augment training data and improve model robustness in domain adaptation. Additionally, recent work in unsupervised domain adaptation has focused on adding variation to the logit for long-tail semantic segmentation with promising results [2]. However, there has been no attention paid to applying noise to pose estimation tasks for regression in UDA research. Our work addresses this gap by introducing variation to domain adaptive pose estimation.

4 PROPOSED SOLUTION

4.1.1 Overview

Our proposed solution is three-fold.

- We implemented an existing state-of-the-art supervised method for capturing noise for UDA [3].
- We proposed adding scaled variation to the keypoint prediction heatmap. By adding scaled variation, we accentuate the heatmap to provide more accurate final key point predictions.
- We experimented with adding scaled variation before the deconvolution layer. This idea is inspired by a recent work focusing on adding variation to logits of long-tailed distributions for semantic segmentation tasks [2].



4.1.2 Figure 2: Illustration of (a) Residual Log-likelihood Estimation for Unsupervised Domain Adaptation, and (b) Adding Scaled Variation to Keypoint Prediction Heatmap.

4.1.3 Residual Log-likelihood Estimation for Unsupervised Domain Adaptation

Li et al. [3] utilized residual log-likelihood (RLE) to estimate the underlying keypoint distribution for supervised human pose estimation. Following their work, we implemented RLE for UDA. However, as seen in Table 1, the result shows no improvement in the UDA setting when compared to the baseline.

RLE is applied to regression-based methods. To the best of our knowledge, there is no heatmap-based method of estimating noise. This led us to propose our method for modelling noise for heatmap-based pose estimation methods, as discussed in the next section.

4.1.4 Scaled Variation for Keypoint Prediction Heatmap

We proposed adding scaled variation to the keypoint prediction heatmap. By adding scaled variation, we sharpen the heatmap to provide more accurate final key point predictions.

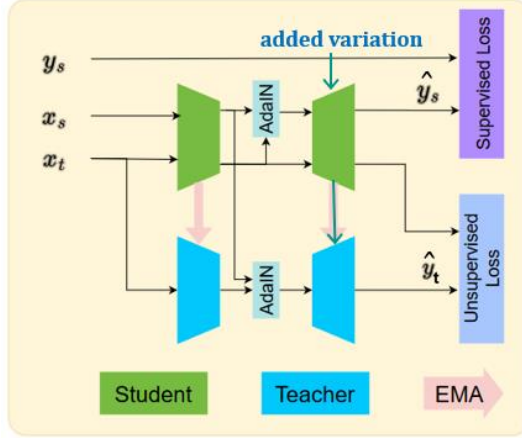
To achieve this sharpening effect, the amount of noise we add is normalized and proportional to the keypoint prediction in the heatmap. Specifically,

$$\hat{h}_i = h_i \frac{h_i}{\sum_{i \in h} h_i} |\delta(\sigma)| \quad (1)$$

where h_i is the i -th pixel of the heatmap, δ is a gaussian distribution with a mean of 0 and standard deviation of σ .

4.1.5 MAV (Our Method)

Our method adds scaled variation to the feature representations before the deconvolution layer. This idea is inspired by a recent work focusing on adding variation to logits of long-tailed distributions for semantic segmentation tasks [2]. Heatmaps can be considered as a long-tailed distribution, where the majority of keypoint predictions are centred around the joint and the remaining ones are scattered further apart. Meanwhile, the deconvolution layers act as non-linearities, similar to the softmax function in the original work [2].



Similar to equation 1), except we now scale with respect to the feature vectors instead of the keypoint predictions heatmap.

To achieve reliable noise reduction in the target domain, two techniques are employed: 1) the latent feature vectors of the source to target images are dynamically adjusted with the mean and variance of the target features via adaptive instance norm, and 2) model weights are updated between the student and the teacher model through exponential moving averaging.

Figure 3: MAV Architecture with Added Variation

5 EXPERIMENT DESIGN

5.1.1 Dataset



We evaluate our MAV pipeline using Synthetic Animal Dataset [14] → TigDog Dataset [15]. This dataset is commonly used in UDA settings [16]. The source domain is synthetic images cropped from online video game simulations. The target images contain complex natural scenes of tigers and horses. This task is challenging and non-trivial.

Figure 4: Synthetic Animal (Top row) → TigDog (Bottom Row)

5.1.2 Augmentations

Following the work of [17], we used random data augmentations. More specifically, we used 60-degree rotations, shear (-30, 30), translations (0.05, 0.05), scaling (0.6, 1.3), and 0.25 contrast.

5.1.3 Architecture

MAV is applied on top of ImSty, a non-parametric feature-level domain alignment method [16]. ImSty is built on top of StyleNet, a common style transfer baseline in domain adaptation [19].

Standard ResNet-101 is used as the backbone and three blocks of upsampling blocks with 256 channels (comprised of 2D transpose convolution, 2D batch norm, and ReLU) are used in the decoder. Source-only pre-training is done for 40 epochs, and the entire network is trained for 70 epochs.

5.1.4 Metrics

For 2D pose estimation, the standard metric is Percentage of Correct Keypoints (PCK). Following the work of Kim et al. [17] and Li & Lee [18], all experiments are reported with PCK@0.05 which measures the ratio of correct key points that are within 5% of the image resolution.

6 RESULTS

Although specifically designed for unsupervised pose estimation, our proposed framework is general and can be adapted to both supervised and unsupervised pose estimation. We benchmarked the proposed method on the Synthetic Animal \rightarrow TigDog dataset, specifically for horses and tigers. With a simple yet effective architecture, our method achieves **76.2** Percentage of Correct Key points at 5% of image resolution for the horse class, 0.7% higher than the previous state-of-the-art method.

Main Results. In Table 1, we compared our method (MAV) with SOTA models for UDA pose estimation on three sets of 2D pose estimation datasets for domain adaptation. Although the SOTA model outperformed our method by 0.4% on the tiger dataset, our model achieved an improvement of **0.7%** for the horse class with minor parameter overheads.

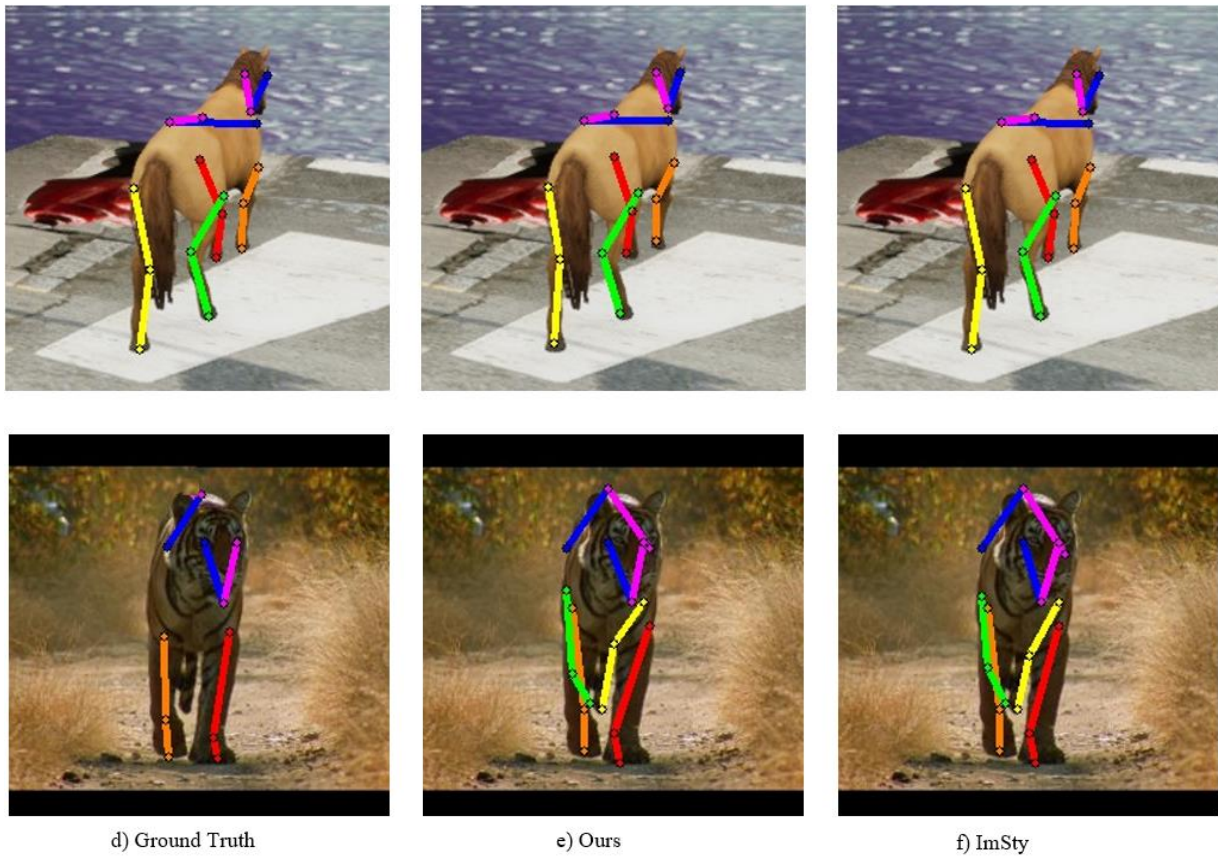


Figure 5. **Qualitative Comparison.** The first row is on the synthetic source domain. The second row is on the real-world target domain. ImSty and our method both achieve 97.4 PCK@0.05 on the

source domain for supervised pose estimation. Our method achieves a +0.7% improvement for unsupervised pose estimation for tigers.

| Method | $PCK@0.05$ Target (Tiger) | $PCK@0.05$ Target (Horse) | Best epoch |
|----------------------------------|------------------------------|------------------------------|------------|
| ImSty | 66.9 (65.8)* | 75.4 | 48 |
| ImSty (RLE) | 64.3 | 73.3 | 53 |
| ImSty ($\sigma=0.002$, scaled) | 65.5 | 75.8 | 65 |
| ImSty ($\sigma=0.002$, MAV) | 65.4 | 76.1 | 63 |

Table 1 **Quantitative Result** ImSty has converged, but MAV has not fully converged yet. Training for a few more epochs may bring better results. *Note: We obtained a slightly different $PCK@0.05$ (in brackets) when re-running ImSty. Most likely, the numbers are slightly different due to differences in seeding.

| Method | Horse ($PCK@0.05$) | | | | | | | |
|--|----------------------|-------------|-------------|-------------|-------------|-------------|-------------|-------------|
| | Eye | Chin | Hoof | Hip | Knee | Shoulder | Elbow | All |
| ImSty | 91.6 | 92.8 | 66.2 | 77.1 | 76.5 | 72.6 | 74.7 | 75.4 |
| ImSty ($\sigma=0.002$, scaled) | 90.8 | 92.1 | 67.9 | 74.7 | 77.8 | 74.1 | 71.3 | 75.8 |
| ImSty ($\sigma=0.002$, MAV) | 91.7 | 92.6 | 67.5 | 78.1 | 78.2 | 73.5 | 72.1 | 76.1 |

Table 2 **Quantitative Result** for horse for each keypoint joint.

| Method | Tiger ($PCK@0.05$) | | | | | | | |
|--|----------------------|-------------|-------------|-------------|-------------|-------------|-------------|-------------|
| | Eye | Chin | Hoof | Hip | Knee | Shoulder | Elbow | All |
| ImSty | 97.7 | 96.3 | 72.1 | 72.5 | 61.3 | 52.9 | 52.2 | 66.9 |
| ImSty ($\sigma=0.002$, scaled) | 97.2 | 95.0 | 69.8 | 65.5 | 62.0 | 51.6 | 48.8 | 65.5 |
| ImSty ($\sigma=0.002$, MAV) | 96.7 | 95.6 | 70.5 | 66.8 | 60.8 | 51.2 | 48.8 | 65.4 |

Table 3 **Quantitative Result** for tiger for each keypoint joint.

6.1.1 Ablations

| Method | <i>PCK@0.05</i> Target (Tiger) | <i>PCK@0.05</i> Target (Horse) | Best epoch |
|---------------------------------------|-----------------------------------|-----------------------------------|------------|
| ImSty | 66.9 (65.8) | 75.4 | 48 |
| ImSty ($\sigma = 0.02$, scaled) | 65.3 | 75.7 | 50 |
| ImSty ($\sigma = 0.02$, MAV) | 65.6 | 75.4 | 60 |
| ImSty ($\sigma = 0.002$, scaled) | 65.5 | 75.8 | 65 |
| ImSty ($\sigma = 0.002$, MAV) | 65.4 | 76.2 | 63 |

Table 4 **Ablations**. Smaller variance ($\sigma = 0.002$) provided more improvements in results than larger variance ($\sigma = 0.02$). MAV also provided more improvements than scaled noise.

7 CONCLUSION AND FUTURE WORK

Our method achieves **76.2% PCK@0.05** for the horse class in the standard synthetic animal to TigDog benchmark. While our model shows no improvement for the tiger class compared to SOTA, it outperforms the state-of-the-art by **+0.7%** for the horse class. Additionally, our ablation studies revealed that reducing the variance leads to greater improvements, and our proposed method, MAV, outperforms adding scaled noise directly to the keypoint heatmap prediction.

7.1.1 Future Work

- Although specifically designed for UDA, our method is architecture-agnostic. It would be interesting to see results from applying MAV to supervised domain adaptation.
- To reduce high variances in both input image and output keypoint settings, we should use more datasets, such as human and hand. Especially existing methods for noise estimation (for example, RLE) are applied to human pose estimation.
- The current model improvement is 0.7%, which is minimal. We may need multiple runs across multiple seeds to see if there are significant improvements.
- Train for more epochs. The current model is trained for 70 epochs. From Table 1 we can see that the best checkpoint happened at epoch 63. We hypothesize that the model takes longer to converge after adding noise, and the model may not have converged yet.

8 REFERENCES

- [1] A. Bulat and G. Tzimiropoulos, “Human pose estimation via convolutional part heatmap regression,” in *Computer Vision–ECCV 2016: 14th European Conference, Amsterdam, The Netherlands, October 11–14, 2016, Proceedings, Part VII 14*. Springer, 2016, pp. 717–732.
- [2] Y. Wang, J. Fei, H. Wang, W. Li, T. Bao, L. Wu, R. Zhao, and Y. Shen, “Balancing logit variation for long-tailed semantic segmentation,” in *Proceedings of the IEEE/CVF Conference on Computer Vision and Pattern Recognition*, 2023, pp. 19 561–19 573.
- [3] J. Li, S. Bian, A. Zeng, C. Wang, B. Pang, W. Liu, and C. Lu, “Human pose regression with residual log-likelihood estimation,” in *Proceedings of the IEEE/CVF international conference on computer vision*, 2021, pp. 11 025–11 034.
- [4] A. Nibali, Z. He, S. Morgan, and L. Prendergast, “3d human pose estimation with 2d marginal heatmaps,” in *2019 IEEE Winter Conference on Applications of Computer Vision (WACV)*. IEEE, 2019, pp. 14771485.
- [5] B. Xiao, H. Wu, and Y. Wei, “Simple baselines for human pose estimation and tracking,” in *Proceedings of the European conference on computer vision (ECCV)*, 2018, pp. 466–481.
- [6] J. Ding, B. Chen, H. Liu, and M. Huang, “Convolutional neural network with data augmentation for sar target recognition,” *IEEE Geoscience and remote sensing letters*, vol. 13, no. 3, pp. 364–368, 2016.
- [7] M. Afifi and M. S. Brown, “What else can fool deep learning? addressing color constancy errors on deep neural network performance,” in *Proceedings of the IEEE/CVF international conference on computer vision*, 2019, pp. 243–252.
- [8] N. Srivastava, G. Hinton, A. Krizhevsky, I. Sutskever, and R. Salakhutdinov, “Dropout: a simple way to prevent neural networks from overfitting,” *The journal of machine learning research*, vol. 15, no. 1, pp.1929–1958, 2014.
- [9] A. Kurakin, I. Goodfellow, and S. Bengio, “Adversarial machine learning at scale,” *arXiv preprint arXiv:1611.01236*, 2016.
- [10] J. Kim, J. Jeong, and J. Shin, “M2m: Imbalanced classification via major-to-minor translation,” in *Proceedings of the IEEE/CVF conference on computer vision and pattern recognition*, 2020, pp. 13 89613 905.
- [11] C. Xie, M. Tan, B. Gong, J. Wang, A. L. Yuille, and Q. V. Le, “Adversarial examples improve image recognition,” in *Proceedings of the IEEE/CVF conference on computer vision and pattern recognition*, 2020, pp. 819–828.
- [12] Q. Lin, K. Gu, L. Yang, and A. Yao, “Synthetic-to-real pose estimation with geometric reconstruction,” *Advances in Neural Information Processing Systems*, vol. 36, 2024.

- [13] L. Huang, Y. Li, H. Tian, Y. Yang, X. Li, W. Deng, and J. Ye, "Semi-supervised 2d human pose estimation driven by position inconsistency pseudo label correction module," in Proceedings of the IEEE/CVF Conference on Computer Vision and Pattern Recognition, 2023, pp. 693703.
- [14] J. Mu, W. Qiu, G. D. Hager, and A. L. Yuille, "Learning from synthetic animals," in Proceedings of the IEEE/CVF Conference on Computer Vision and Pattern Recognition, 2020, pp. 12 386–12 395.
- [15] L. Del Pero, S. Ricco, R. Sukthankar, and V. Ferrari, "Articulated motion discovery using pairs of trajectories," in Proceedings of the IEEE Conference on Computer Vision and Pattern Recognition (CVPR), 2015.
- [16] J. Park, F. Barnard, S. Hossain, and S. Rambhatla, "Implicit stylization for domain adaptation," 2023.
- [17] D. Kim, K. Wang, K. Saenko, M. Betke, and S. Sclaroff, "A unified framework for domain adaptive pose estimation," in European Conference on Computer Vision. Springer, 2022, pp. 603–620.
- [18] C. Li and G. H. Lee, "From synthetic to real: Unsupervised domain adaptation for animal pose estimation," in Proceedings of the IEEE/CVF conference on computer vision and pattern recognition, 2021, pp. 14821491.
- [19] C. Gan, Z. Gan, X. He, J. Gao, and L. Deng, "Stylenet: Generating attractive visual captions with styles," in Proceedings of the IEEE conference on computer vision and pattern recognition, 2017, pp. 31373146.